

SYNCHROTRON EMISSION FROM THE GALACTIC HI LAYER

Yonggi Kim^{1,2†} and Jun-Young Oh²

¹University Observatory, Chungbuk National University, Cheongju 361-763, Korea

²Institute for Basic Science Research, Chungbuk National University, Cheongju 361-763, Korea
email: ykkim153@chungbuk.ac.kr

(Received January 31, 2007; Accepted February 3, 2007)

ABSTRACT

The relationship between the Galactic magnetic field strength and the gas density has been revisited. A synchrotron continuum emission data at 408 MHz and HI column density provide a good data for such study. But it is difficult to separate the synchrotron emission from the observed 408MHz radio emission, because the 408MHz radio emission has the component from the HI layer, as well as many components from other origins. We have tried to subtract the component which is probably not related with HI layer, and present the results. We show that the method presented here is a more refined method than that of Brown & Chang (1983, hereafter BC83) to find the above mentioned relationship, and discuss the existence of such relationship in our Galaxy.

Keywords: ISM, HI layer, magnetic fields, radio continuum

1. INTRODUCTION

The magnetic field is strongly related with the interstellar medium (ISM). The magnetic field distribution in the ISM provides a significant information about its structure as well as the distribution and propagation of cosmic rays. Mouschovias (1985) showed that the magnetic field B seems to scale with the gas density according to $B = B_i(n/n_i)^k$, where a range for the exponent lies in $1/3 \leq k \leq 1/2$ and the index i corresponds to the initial situation. Troland & Heiles (1982) suggested in the study of the Zeeman effect that the theoretical argument about the above density dependence is incorrect. According to their conclusion, the magnetic field is unlikely to play an important role in influencing large-scale motions of the gas due to the low magnetic energy densities in the regions of $0.1 \leq n(\text{cm}^{-3}) \leq 10^2$. However Fleck (1983) showed that this “B versus n dilemma” can be resolved in terms of preferential mass flow along magnetic field lines as a result of an increase in the ratio of magnetic and gas pressure.

BC83 presents an exponent k of 0.44 in another approach, which the observations of the non-thermal galactic background component at 327 MHz are compared with the 21 cm HI emission. Their results encountered a strong criticism from Troland & Heiles (1986, hereafter TH86). TH86 suggested no increase in field strength for particle densities $n \leq 100\text{cm}^{-3}$. Recently Kim (2000) summarized this discussion about the B-n problem, and carried out similar study to BC 83, but with improved method. He adopted the suggestion of Beuermann, Kanbach, & Berkhuijsen (1985, hereafter BKB) who noted that a fraction of the nonthermal continuum emission at 408 MHz (Haslam et

[†]corresponding author

al. 1982) is connected with the HI cloud. He concluded that there is in fact a well defined nonthermal component at 408 MHz which is correlated with the HI column density and originates from this HI layer.

As Berkhuisen, Bajaja, & Beck (1993) presented, studies of the relationship between properties of the magnetic field and of the gas in large clouds can be made by comparing the nonthermal radio continuum emission with that of HI and CO in order to obtain orientation and strength of the magnetic field as well as the distribution and density of the neutral gas. To do such study, it is very important to get the real part of the nonthermal radio continuum emission as exactly as possible. In this paper, it is therefore focused on the method to subtract the component which is probably not related with HI layer from the observed 408 MHz radio emission.

2. DATA STRUCTURE AND REDUCTIONS

The nonthermal radio emission data can be provided by the Bonn all sky survey (Haslam et al. 1982) which has a resolution of $0.^\circ85$ and gives the brightness temperature at 408 MHz (K) in a grid of 1° interval of the galactic latitude and the galactic longitude. BKB presented a three-dimensional model of the Galactic radio emission at 408 MHz, showing that the Galaxy consists of a thick nonthermal radio disk in which a thin disk is embedded. In this model extended low density (ELD) HII regions, old supernova remnants and synchrotron emission from an HI cloud are suggested as possible constituents of the thin disk. Fig. 1 shows an observed latitude distribution of the 408 MHz brightness temperature and the column density of the neutral hydrogen at $l = 322^\circ$ (upper and lower solid curve respectively).

BKB model suggests $2.6 \times 10^{20} \text{WHz}^{-1}$ as the total radiation power for the HI cloud component at 408 MHz. With total mass of galactic HI, $2.6 \times 10^9 M_\odot$ (Baker & Burton 1975), the averaged synchrotron emissivity for the HI cloud at 408 MHz can be estimated:

$$\varepsilon_{\text{HI}} = 4n \text{ Kkpc}^{-1} \quad (1)$$

The isotrope emission is assumed here ($1 \text{Kkpc}^{-1} = 1.65 \times 10^{-2} \text{Wm}^{-3} \text{Hz}^{-1} \text{sr}^{-1}$) and n is the averaged particle density in the HI cloud in unit of H-atoms cm^{-3} . The expected brightness temperature from the HI component can be now obtained:

$$\begin{aligned} T_{b,HI} &= \frac{\varepsilon_{\text{HI}} \times L}{3.086 \times 10^{21}} \\ &= 1.3 \times 10^{-21} N_{\text{HI}} \end{aligned} \quad (2)$$

where L is the length integrated along the line of sight in the HI cloud. In the lower panel of Fig. 2 we show longitude profiles for the observed $T_b(408)$ (upper curve), the background component(lower curve) and the sum of the background component and the expected HI component(middle curve). Because of the contamination of another components in the brightness temperature, the correlation between $T_b(408)$ and N_{HI} would have a form:

$$\begin{aligned} T_b(408) &= T_{b,B} + T_{b,HI} \\ &= A + BN_{\text{HI}} \end{aligned} \quad (3)$$

Eq. 3 holds only if $T_b(408)$ has no contributions of thermal radiation and nonthermal discrete sources and in this case, $T_{b,B}$ corresponds to the contribution of the thick radio disk in BKB model (background component). Therefore the regions where are contaminated in the strong radio sources, are

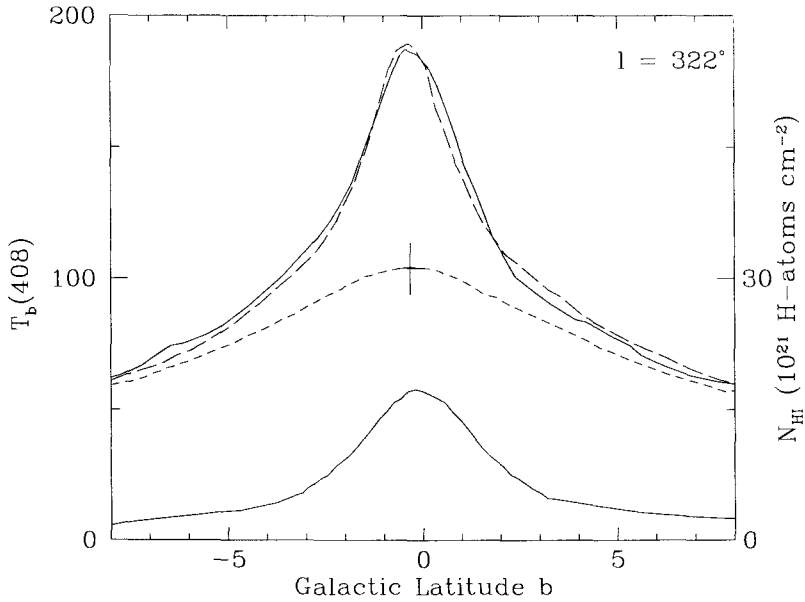


Figure 1. Observed latitude distribution of the 408 MHz brightness temperature and N_{HI} at $l = 322^\circ$ (upper and lower solid line respectively). Two components of the radio disk according to BKB model are also illustrated in this figure (short dashed and long dashed for the thick and the sum of thin and thick component respectively).

not suitable to carry out such correlation study. These regions must be excluded from the further analysis in our study in contrast to BC83 who used all data in the whole Galaxy in a similar study to ours. The regions not suitable in our analysis are chosen as follows:

With help of the catalog of galactic HII regions (Blitz, Fich, & Stark 1982) and lists of supernova remnants the distribution of these sources have been made in region of $50^\circ < l < 250^\circ$ and $-10^\circ < b < +10^\circ$ and illustrated as a circle in the middle panel of Fig. 2. The diameter of the circle corresponds to the optical diameter of these sources. This figure shows that many HII regions and supernova remnants are in the region of $l < 145^\circ$

The influence of radio sources on the observed brightness temperature along the galactic disk can be roughly estimated by comparing the longitudinal profile of the observed and expected brightness temperatures with the HI cloud. The contribution of the thin radio disk has the greatest value at the ridge line where the radio continuum indicates its maximum at the latitude profile as the Fig. 1 shows. The upper curve in the lower panel of Fig. 2 represents the longitudinal profile of the observed $T_b(408)$ at the ridge line in units of Kelvin. The lower curve in this panel shows the background component at the ridge line and the middle one corresponds to the expected HI component estimated by Eq. 3. Although this estimate is somewhat rough, the observed brightness temperature seems to be correlated with the expected brightness temperature from HI cloud. From this panel it is very easy to see where the observed T_b is strongly influenced by the radio sources (for example in the Cygnus region near $l = 80^\circ$, in supernova remnant Cas A near $l = 120^\circ$, and in Rosetta nebular near $l = 205^\circ$). A comparison study in such region is impossible. But in the region where $T_{b,B} + T_{b,HI}$ approaches

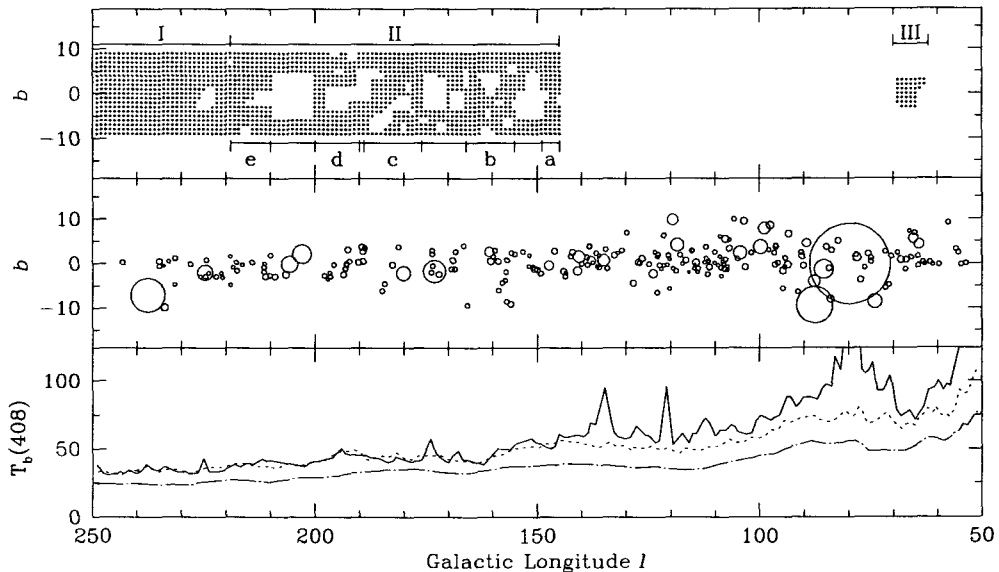


Figure 2. Overview of the galactic disk for $50^\circ < l < 250^\circ$: the upper panel indicates regions used for $T_b(408) - N_{\text{HI}}$ correlation, the middle panel the distribution of HII regions and supernova remnants, and the lower panel shows longitude profile of $T_b(408)$ (solid), the HI component (dotted) expected by BKB model and background component (dot dashed) at the ridge line.

to $T_b(408)$, one can say that $T_b(408)$ is not influenced by the sources and thus the $T_b(408) - N_{\text{HI}}$ correlation study can be undertaken.

The region at $l < 145^\circ$ shows also an example for the region strongly influenced by the sources. Here we can not find no suitable region except of the region near $l = 65^\circ$. The region of $145^\circ < l < 220^\circ$ exhibits a suitable region for the $T_{b,B} + T_{b,HI}$ relationship study, except of some regions with strong sources. However it is difficult to remove such strong thermal and nonthermal sources from the total brightness temperature. Another possible region for such study reveals again in region of $220^\circ < l < 250^\circ$. There are in this region no strong sources as in the region $145^\circ < l < 220^\circ$.

Consequently the region of $220^\circ < l < 250^\circ$ and $-10^\circ < b < +10^\circ$ is selected as region I. In this region there are no supernova remnants and no strong HII regions except of RCW 1 near $l = 225^\circ$. RCW 1 region is excluded in the further analysis, because the contribution of this region can be estimated not sufficiently. The big HII region RCW 15 near $l = 235^\circ$ in the middle panel of Fig. 2 is a ELD HII region. It has a big diameter, but the thermal contribution to the observed brightness temperature amounts only about 1 K so that this region can be used to be analyzed after a careful correction.

As a region II we define the region of $145^\circ < l < 220^\circ$ and $-10^\circ < b < +10^\circ$. The curves of $T_b(408)$ and $T_{b,B} + T_{b,HI}$ run parallel together, but the correlation study may be disturbed by the many radio sources. Because of the difficulty of the correction, some regions influenced by

radio sources are excluded in the further study. As the lower panel of Fig. 2 shows, the background component becomes greater with small galactic longitude. In order to avoid the problem arisen by such varying background component, region II is divided into 5 part regions in which $T_{b,B}$ seems to be constant.

A small region of $62^\circ < l < 70^\circ$ and $-4^\circ < b < +4^\circ$ is selected as region III. In region between the Sagittarius arm at $l = 50^\circ$ and the local arm at $l = 70^\circ$ the radio emission becomes weaker again, which enables the correlation study. All grid points of the galactic longitude and latitude which are used in this study are marked by * in the upper panel of Fig. 2.

We showed above a possible existence of the $T_b(408) - N_{\text{HI}}$ correlation with the expected HI component by BKB model. It can be now directly tested this correlation by using the observed $T_b(408)$ and N_{HI} in Eq. 3. This is the main purpose of this paper. The velocity integrated HI column density to be used in Eq. 3 can be obtained by Weaver & Williams (1973) and Bloemen (1983). This column density is also available in a grid of 1° interval of the galactic latitude and the galactic longitude as $T_b(408)$.

Before undertaking this test, the contribution of the radio sources in $T_b(408)$ must be corrected carefully as possible. For this correction, the radiation flux of radio sources with $S \geq 2$ Jy at 408 MHz is selected, and has been transformed to the brightness temperature at 408 MHz in Kelvin:

$$T_b(408) = 0.78 \times S \quad (4)$$

This temperature is a peak temperature which is observed at the position of the radio source. Because $T_b(408)$ and N_{HI} grids of 1° interval are used in this paper, the contribution of this radio source to the brightness temperature at a neighboring grid is to be estimated by using Gauss distribution.

Some thermal radio sources which are identified in the 1420 MHz survey as discrete sources (Reich & Reich 1986) contribute also to the brightness temperature at 408 MHz. This contribution can be expressed by

$$\begin{aligned} T_b(408) &= T_b(1420) \left(\frac{\theta_{1420}}{\theta_{408}} \right)^2 \left(\frac{1420}{408} \right)^{2.1} \\ &= 6.61 T_b(1420). \end{aligned} \quad (5)$$

ELD HII regions have lower emission measure due to their lower density. A typical value for emission measure EM amounts for ELD HII regions in spiral galaxy between 30 and 50 cm^{-6} pc (Mezger 1978). For the individual observed ELD HII regions at $220^\circ < l < 240^\circ$ the emission measure lies between 4 and 60 cm^{-6} pc (Reynolds, Roesler, & Scherb 1974). The brightness temperature for a thermal plasma with the electron temperature T_e and the electron density N_e is given by

$$T_b(408) = 8.235 \times 10^{-2} a(\nu, T_e) T_e^{-0.35} \nu^{-2.1} EM \quad (6)$$

where T_e in unit of Kelvin and ν in unit of GHz. This contribution at a neighboring grid is also estimated by using Gauss distribution.

All values of the various contributions estimated above are subtracted from the total $T_b(408)$ in the corresponding grid. In the rest of this paper $T_b(408)$ means the corrected brightness temperature.

3. $T_b(408) - N_{\text{HI}}$ CORRELATION

The least square method has been used to find the linear correlation (Eq. 3) between the corrected brightness temperature and a HI column density at the grid of regions. We summarize here the results of each region.

Table 1. Results in region I for $T_b(408) = A + B N_{\text{HI}}$ in a given latitude region. $T_b(408)$ and A is in unit of Kelvin and N_{HI} is in unit of $10^{21} \text{H} - \text{atoms cm}^{-2}$. R is a linear correlations coefficient.

Latitude	A	B	R
$-10 \leq b' \leq +10$	23.02 ± 0.18	1.38 ± 0.03	0.865
$-4 \leq b' \leq +4$	23.52 ± 0.53	1.27 ± 0.08	0.717
$5 \leq b' \leq +8$	23.76 ± 0.53	1.27	
$-8 \leq b' \leq -5$	23.86 ± 0.64	1.27	
$9 \leq b' \leq +11$	22.42 ± 0.75	1.27	

3.1 Region I

Using all data in region I we found a linear relationship:

$$T_b(408) = (23.02 \pm 0.16) + (1.38 \pm 0.03)N_{\text{HI}} \quad (7)$$

As Fig. 1 shows, the background component varies with the galactic latitude, *i.e.* the value of A in Eq. 3 changes in the course of the galactic latitude. Therefore it is appropriate to separate the data by the galactic latitude. Because the ridge line b_R varies in the galactic longitude, we introduce a shift galactic latitude, $b' = b + b_R$, where b_R in region I is -2° .

We examined, at first, the correlation for the galactic disk, $|b'| \leq 4^\circ$. The values found here are listed in Table 1. This result is consistent with the result for the all data given by Eq. 7. It can be argued that the slope of B is independent (or little dependent) on the latitude. Thus we assumed that the slope $B = 1.27$ holds for all galactic latitude in region I, and forward to search a better estimate of A for $|b'| > 4^\circ$. For several regions with different latitude interval the value A is found with the fixed $B = 1.27$ and their results are listed also in Table 1. We can see a background component being almost constant in the course of galactic latitude. Only for $b' \geq 9$, a weak decrease in A is found, which leads to the high value of B in Eq. 7. In Fig. 3 we find also the $T_b(408) - N_{\text{HI}}$ correlation for some latitude region. The slope gives a found value of B listed in Table 1.

3.2 Region II and III

After a detailed study in region I, the $T_b(408) - N_{\text{HI}}$ correlation in the region II and III has been also carried out. The values of A and B found by this method are listed in Table 2. These values seems to be not bad, but the correlation coefficient is only 0.582, more worse than in region I ($R=0.865$). The poor correlation in region II is perhaps caused by the fact that the A in Eq. 3 varies slightly along the galactic longitude as we saw in Fig. 2. We divided the region II in 5 part regions as marked in Fig. 2. Since it has been shown in the previous subsection that the correlation at $|b'| \leq 4$ is representative in region I and the background component seems to vary at smallest in this latitude region, the 5 part regions at $|b'| \leq 4$ are chosen for the further study.

A study of these part regions provides immediately a good correlation for IIa, IIc and IIe regions compared with the poor correlation for the whole region II. The slope B found here is comparable with the value for the region I. The results of these part regions listed also in Table 2 show that the value of A is in fact very different along the galactic longitude as Fig. 2 also indicates.

It is shown that the part region IIb can be divided also in 2 regions with a different background component. 2 regions for $0^\circ < b' < 4^\circ$ and $-4^\circ < b' < -1^\circ$ are selected, and a good correlation is found for these regions. The results are listed in Table 2. The slope B is high yet for $-4^\circ < b' < -1^\circ$ and therefore the correlation study for $N_{\text{HI}} \geq 5.5 \times 10^{21} \text{H} - \text{atoms cm}^{-2}$ has been undertaken. It's result leads to a similar slope to that for $0^\circ < b' < 4^\circ$.

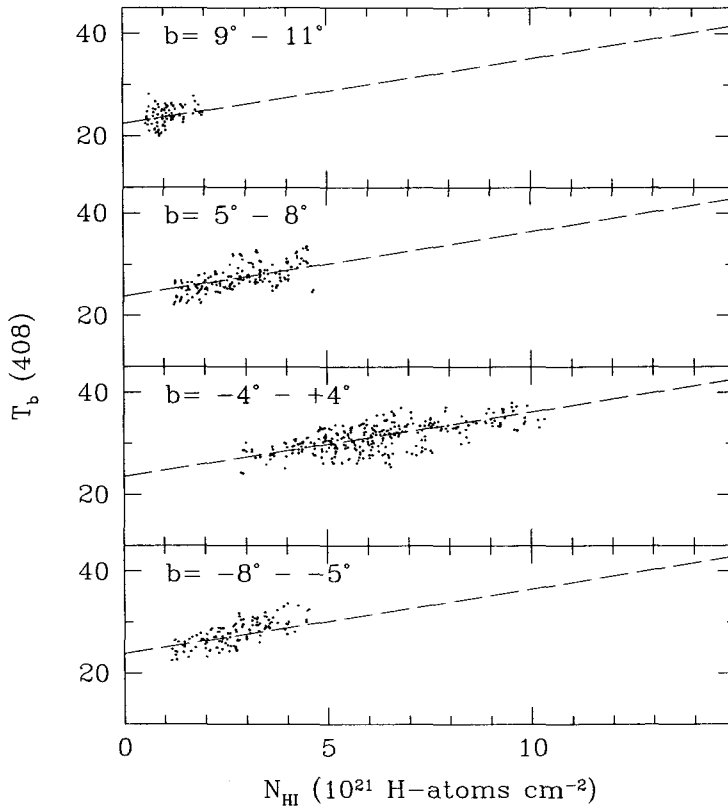


Figure 3. The $T_b(408) - N_{\text{HI}}$ correlation for some latitude in region I. The slope in each correlation is listed in Table 1.

More extreme is the situation in region IIc in which a correlation study provides an anticorrelation with $R = -0.199$. A geometric division in 2 part region symmetrically to the galactic plane made possible, however, to get two clear correlation with positive slope and different background component. We find two different structure in $T_b(408) - N_{\text{HI}}$ correlation. There are also some grid points (at $b' = 0^\circ$), for which it is uncertain to which structure they belong. We have excluded these points in the correlation study. For some grid point, it is impossible to estimate the contribution of the radio source. They are not included in the correlation study. We found that this region has obviously not constant background component.

The correlation study for region II has shown how difficult is to carry out a correlation study in our Galaxy. It is impossible to undertake such study in wide region of galactic latitude and longitude, but the disturbing influence of the background component must be examined carefully in each region. This is a essential reason why the similar analysis of BC83 is regarded as incorrect.

Finally, the correlation in a small region near $l = 65$ (region III) has been also found. Here we have excluded all grid points which seem to be highly influenced by radio sources. A good

Table 2. Results in region II and III for $T_b(408) = A + B N_{\text{HI}}$ in a given latitude region. $T_b(408)$ and A are in Kelvin and N_{HI} is in units of $10^{21} \text{H} - \text{atoms cm}^{-2}$. R is the linear correlation coefficient. In the region marked with * only the $N_{\text{HI}} \geq 5 \times 10^{21}$ has been used for the correlation study.

Region	l	b'	A	ΔA	B	ΔB	R
II	145 - 219	-10 - +10	28.8	± 0.36	1.63	± 0.07	0.582
II	145 - 219	-4 - +4	36.66	± 1.23	0.84	± 0.16	0.201
IIa	145 - 149	-4 - +4	41.04	± 0.98	0.96	± 0.12	0.813
IIb	155 - 166	-4 - +4	33.98	± 0.94	1.52	± 0.14	0.746
		0 - +4	28.94	± 1.38	2.03	± 0.18	0.849
		-4 - -1	24.92	± 1.22	3.64	± 0.25	0.915
		-4 - -1*	35.07	± 1.96	2.04	± 0.30	0.939
IIc	176 - 189	-4 - +4	41.81	± 1.57	-0.33	± 0.20	-0.199
		1 - +4	24.55	± 1.30	1.43	± 0.14	0.837
		-4 - -1	33.80	± 1.59	1.73	± 0.28	0.725
IIId	190 - 200	-4 - +4	33.02	± 0.85	1.04	± 0.12	0.751
IIe	210 - 219	-4 - +4	24.95	± 1.14	1.37	± 0.15	0.727
III	62 - 70	-4 - +4	51.90	± 1.87	1.78	± 0.16	0.897

correlation can be found with $R = 0.897$:

$$T_b(408) = (51.90 \pm 1.87) + (1.78 \pm 0.16)N_{\text{HI}} \quad (8)$$

The value of the background component in this equation, 51.90 is also agreed good with the value estimated with BKB model.

4. CONCLUSIONS

Our results of the $T_b(408) - N_{\text{HI}}$ correlation are illustrated in Fig. 4 where the parameters A and B of Eq. 3 are presented only for $-4^\circ \leq b' \leq +4$. With help of this figure our new findings can be summarized as follows:

1. A correlation of $T_b(408)$ with N_{HI} is found everywhere along the galactic plane as BKB model suggest. The background component A of Eq. 3 is typically stronger than the HI component. The quantity A increases systematically along the galactic plane. B is in the range 1.0 - 2.0 with a mean value of 1.4 ± 0.3 .
2. The correlation is dependent on the direction of observation. The background component varies strong along the galactic plane and is almost constant in a small region. Therefore a correlation study in all region at once is erroneous.
3. $T_b(408)$ correlates good with $N_{\text{HI}} \geq 3 \times 10^{21} \text{H-atoms cm}^{-2}$. The poor correlation for small N_{HI} is probably caused by the variation of the background component.
4. Given the synchrotron emissivity of the near-solar electron spectrum at 408 MHz, $\epsilon = (0.34 \pm 0.09)H_{\perp}^{1.8} \text{Kkpc}^{-1}$ (BKB) and assuming the density of the relativistic electrons to be constant, we obtain for the mean line of sight values of the HI component

$$\langle B_{\perp}^{1.8} \rangle = (12.7 \pm 4.2) \langle n \rangle \quad (9)$$

with B_{\perp} in μG and n in H-atoms cm^{-3} as presented by Kim (2000).

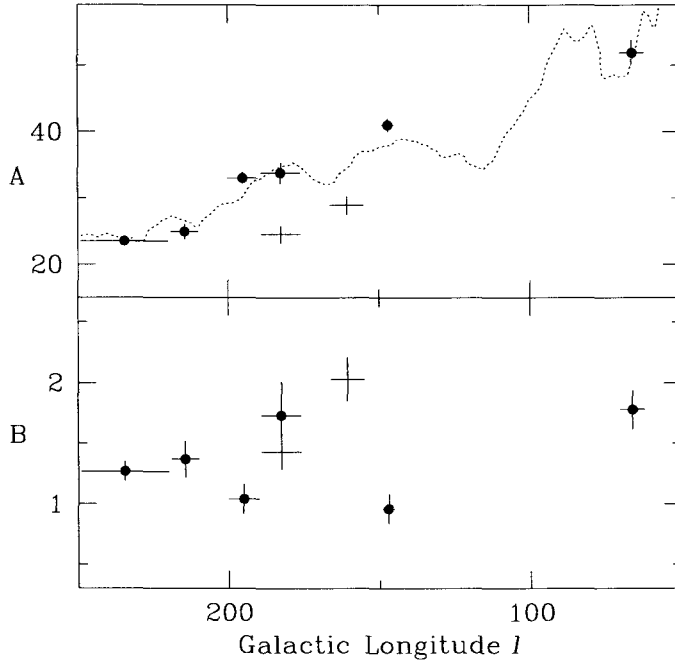


Figure 4. Results of the $T_b(408) - N_{\text{HI}}$ correlation for individual fields within $\pm 4^\circ$ of the ridge line in galactic latitude. The thick component expected by BKB is also illustrated in the upper panel as the dotted curve.

Our results of $T_b(408) - N_{\text{HI}}$ correlation suggest clearly the existence of the relationship between the magnetic field strength and the neutral gas density. It is however to be mentioned that our results hold only for the integrated $T_b(408)$ and N_{HI} in the line of sight. More detailed theoretical and observational studies are highly necessary to solve this “B versus n dilemma”. The method how to separate the nonthermal component of the brightness temperature, and to get the most probable $T_b(408)$, presented in this paper, can be now used to such studies in the future.

ACKNOWLEDGEMENTS: This work was supported by the research grant of the Chungbuk National University in 2006.

REFERENCES

- Baker, P. L. & Burton, W. B. 1975, *ApJ*, 198, 281
 Berkhuijzen, E. M., Bajaja, E., & Beck, R. 1993, *A&A*, 279, 359
 Beuermann, K., Kanbach, G., & Berkhuijzen, E. M. 1985, *A&A*, 153, 17 (BKB)
 Blitz, L., Fich, M., & Stark, A. 1982, *ApJ Supl.*, 49, 183
 Bloemen, J. B. G. M. 1983, in *Surveys of the southern galaxy*, eds. W. B. Burton & F. P. Israel (Reidel: Dordrecht), p.306

- Brown, R. L. & Chang, C.-A. 1983, *ApJ*, 264, 134 (BC83)
Fleck, R. C. 1983, *ApJ*, 264, 139
Haslam, C. G. T., Salter, C. J., Stoffel, H., & Wilson, W. E. 1982, *A&A*, 47, 1
Kim, Y. 2000, *JA&SS*, 17, 33
Mezger, P. G. 1978, *A&A*, 70, 565
Mouschovias, T. Ch. 1985, *A&A*, 142, 41
Reich, P. & Reich, W. 1986, *A&A Supl.*, 63, 205
Reynolds, R. J., Roesler, F. L., & Scherb, F. 1974, *ApJ*, 192, L53
Troland, T. H. & Heiles, C. 1982, *ApJ*, 252, 179
Troland, T. H. & Heiles, C. 1986, *ApJ*, 301, 339 (TH86)
Weaver, H. F. & Williams, D. R. W. 1973, *A&A Supl.*, 8, 1